Scaling Effects in Laser-Based Additive Manufacturing Processes

Andrew J. Birnbaum and Jack L. Beuth
Department of Mechanical Engineering
Carnegie Mellon University
Pittsburgh, Pa 15213

James W. Sears
Advanced Materials Processing Center
South Dakota School of Mines and Technology
Rapid City, SD 57701

Abstract

Thermal modeling is used to address the control of melt pool size in laser-based additive powder fusion processes under steady state conditions. These processes use localized melting of metal powder to add features to metallic components during manufacture or repair. The problem of process size scale is considered, with the aim of applying knowledge developed at one size scale (e.g. the LENS^{TM} process, using a 500 W laser) to similar processes operating at larger scales (e.g. a 3 kW system under development at South Dakota School of Mines and Technology). Results presented herein provide engineers with a means for easily predicting melt pool size for both of these processes over the full range of process variables. Results also demonstrate how process size scale affects the sensitivity of melt pool size to minor changes in process parameters. These issues are addressed via a process map approach developed by the authors and co-workers. This approach collapses results from a large number of simulations over the full range of practical process variables onto plots process engineers can easily use.

Introduction

Recently, the use of laser-based powder fusion processes for component repair and additive manufacturing applications has received significant attention in the aerospace industry. In the case of additive manufacturing, significant cost savings are possible in the fabrication of some components if laser-based deposition is used to add small features to larger parts manufactured by traditional processes. For such applications, process scaling has emerged as a critical issue. Many industrial additive manufacturing applications demand the use of large-scale deposition processes; yet significant process development has taken place on small-scale processes. This includes an extensive research effort over the past eight years at Sandia National Laboratories to develop the LENS^{TM} process (Griffith et al., [1]). Most LENS^{TM} process development research has been performed using a 500 W Nd:YAG laser. In contrast, AeroMet, which manufactures components for the aerospace industry, uses an 18 kW CO_2 laser.

There is currently no fundamental understanding of how to apply knowledge of small-scale systems to analogous large-scale systems. The result is that whenever a new laser-based manufacturing system is developed at a different size scale, processing engineers must nearly start from scratch, performing large numbers of experiments to characterize their specific process. The research described in this paper attempts to address this issue as it relates to steady-state melt pool size control. Work described herein builds directly on modeling work by Vasinonta et al. [2, 3, 4] which developed easy-to-use "process maps," allowing the prediction of steady-state melt pool size in thin walled structures and bulky parts for any practical combination

of LENS^{TM} process variables. A brief overview of the process map approach to understanding laser-based freeform fabrication processes is given by Beuth and Klingbeil [5] and a complete presentation of the process map approach for controlling steady-state melt pool size and residual stress is given by Vasinonta [6]. Most recently, process maps of cooling rates and thermal gradients at the melt pool boundary have been developed with the goal of predicting microstructure (Bontha and Klingbeil, [7]). With the exception of a preliminary consideration of process scaling provided in reference [7], results from this earlier work are tailored for application to the LENS^{TM} or other similarly sized processes.

The work described herein establishes an approach for predicting melt pool size for processes operating at different scales. It builds on work first reported by Birnbaum et al. [8] which presented a preliminary analysis of process scaling limited to the consideration of thin-walled structures. In this paper, a more complete consideration of the deposition of thin-walled structures is given, followed by an analogous consideration of the deposition of bulky features. All of the results presented herein relate to the prediction of steady-state melt pool size. No information is given on the rate of change of melt pool size (from one steady-state value to another) if process variables are altered. Modeling of transient changes in melt pool size is addressed by Birnbaum et al. [8] and Aggarangsi et al. [9]. Although the approach taken is applicable to the laser fusion of any material, research described in this paper will specifically address the deposition of stainless steels.

Numerical Models and the Process Map Approach

Numerical Models: The issues addressed in this research are considered with reference to the part geometries shown in Figure 1. The first geometry represents a thin-walled structure deposited onto a comparatively large base plate that acts as a heat sink. The second geometry represents a bulky structure also deposited onto a large base plate. For both geometries, thermal models are of a concentrated heat source moving across the top of the structure and do not model the effects of material addition. The absorbed laser power is designated as αQ, where α is the fraction of laser power from the source that is absorbed by the structure.

The models used in this paper are analogous to those developed by Vasinonta [6]. For the thin-walled geometry, in comparing with experiments and in determining ranges of absorbed laser powers, a value of $\alpha = 0.35$ is used. For the bulky part geometry, a value of $\alpha = 0.70$ is used. Predictions from numerical models assuming these values of α have shown good agreement with melt pool sizes measured via thermal imaging using the LENS^{TM} process (Vasinonta et al., [2, 6]). In both types of models, the successive deposition of layers is not modeled, but the preheating effects of the deposition of prior layers can be approximated via the specification of an elevated uniform temperature in the part and base plate, designated as T_{base}, which exists before the laser begins its travel across the top of the part.

In all cases considered in this paper, the part is tall enough such that any increases in height will not change the results. The issue of sufficient part heights to achieve this condition is also addressed by Vasinonta et al. [2, 3] and Vasinonta [6]. Similarly, in this study, melt pool size results are taken when the heat source is sufficiently far from the vertical free edges such that results are independent of the distance from the edges. The modeling of changes in melt pool size as a free edge is approached is addressed by Aggarangsi, Beuth and Griffith [10]. In

the process scaling simulations, processes using large values of laser power were performed with models having dimensions scaled up to ensure that the conditions described above were satisfied.

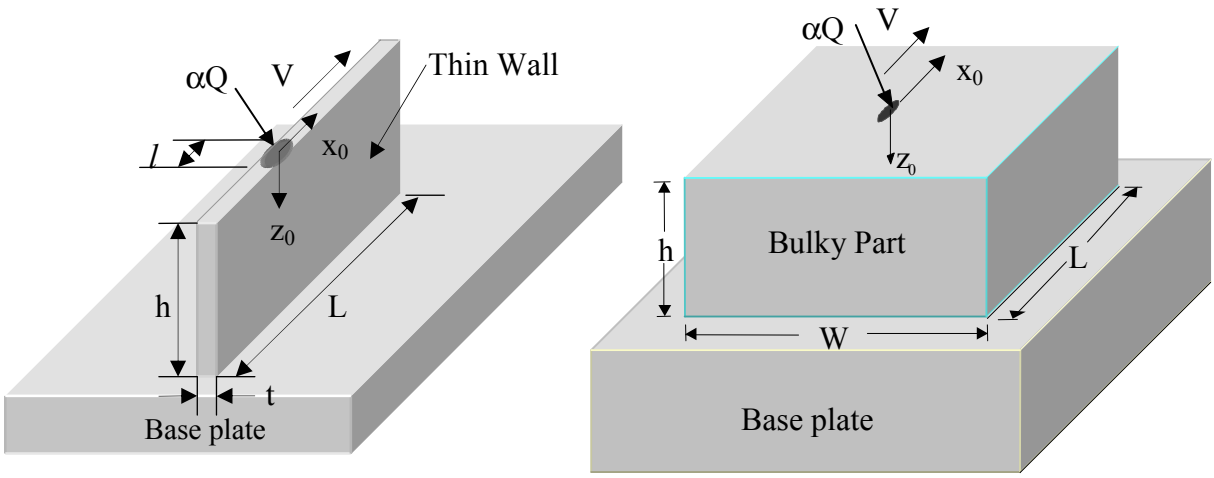

Figure 1 Deposited Geometries with a Base Plate

Figure 2 shows typical finite element meshes used for the scaling effects analyses. For the 2-D analysis of a thin-walled structure, boundary conditions are thermal insulation on the vertical free edges and the top edge, while a constant temperature is enforced at the bottom edge, simulating the effects of the base plate. The models use four-node quadrilateral bi-linear elements provided by the ABAQUS finite element package. Models contain approximately fifteen thousand elements. However, traveling in the direction of the heat source (left to right), there are two separate mesh densities. The first third of the model has fairly coarse resolution, while the remaining portion is of significantly finer resolution. This approach was taken to reduce analysis time with the caveat that fine resolution is only required where melt pool lengths are extracted from the model. Element lengths in the region where melt pool lengths are extracted are small enough that there are always at least ten elements within the melt pool. Mesh resolution also increases as the top edge of the model is approached. Constant power is applied to individual nodes for a time interval equal to the element edge length divided by V.

The mesh used for the bulky part simulations is analogous to that used to model thin walls, except an axisymmetric condition is applied about the axis parallel to the direction of laser travel (designated as the z axis in Fig. 2). Use of an axisymmetric model allows a drastic reduction in computation time compared to an analogous 3-D model. The axisymmetric model actually simulates the movement of a heat source through the center of a large solid (modeling double the volume of the actual geometry). Thus, the applied power used in the simulations was twice that suggested by a value of $\alpha = 0.70$.

Thermal properties of AISI 304 stainless steel are used as inputs to the models (Dobranich and Dykhuizen, [11]). A solidus temperature of 1672 K, a liquidus temperature of 1727 K, a latent heat of fusion of 2.65 x 10^5 J/kg, and a constant density of 7652 kg/m^3 are specified. Below a temperature of 1500 K temperature dependent thermal conductivity, k and specific heat, c are given by the following linear equations:

$$k = 8.116 + 0.01618(T)\ (W/mK) \quad (1)$$
$$c = 465.4 + 0.1336(T)\ \ (J/kgK)\ .$$

Above 1500 K, both thermal conductivity and specific heat are held constant at the 1500 K value.

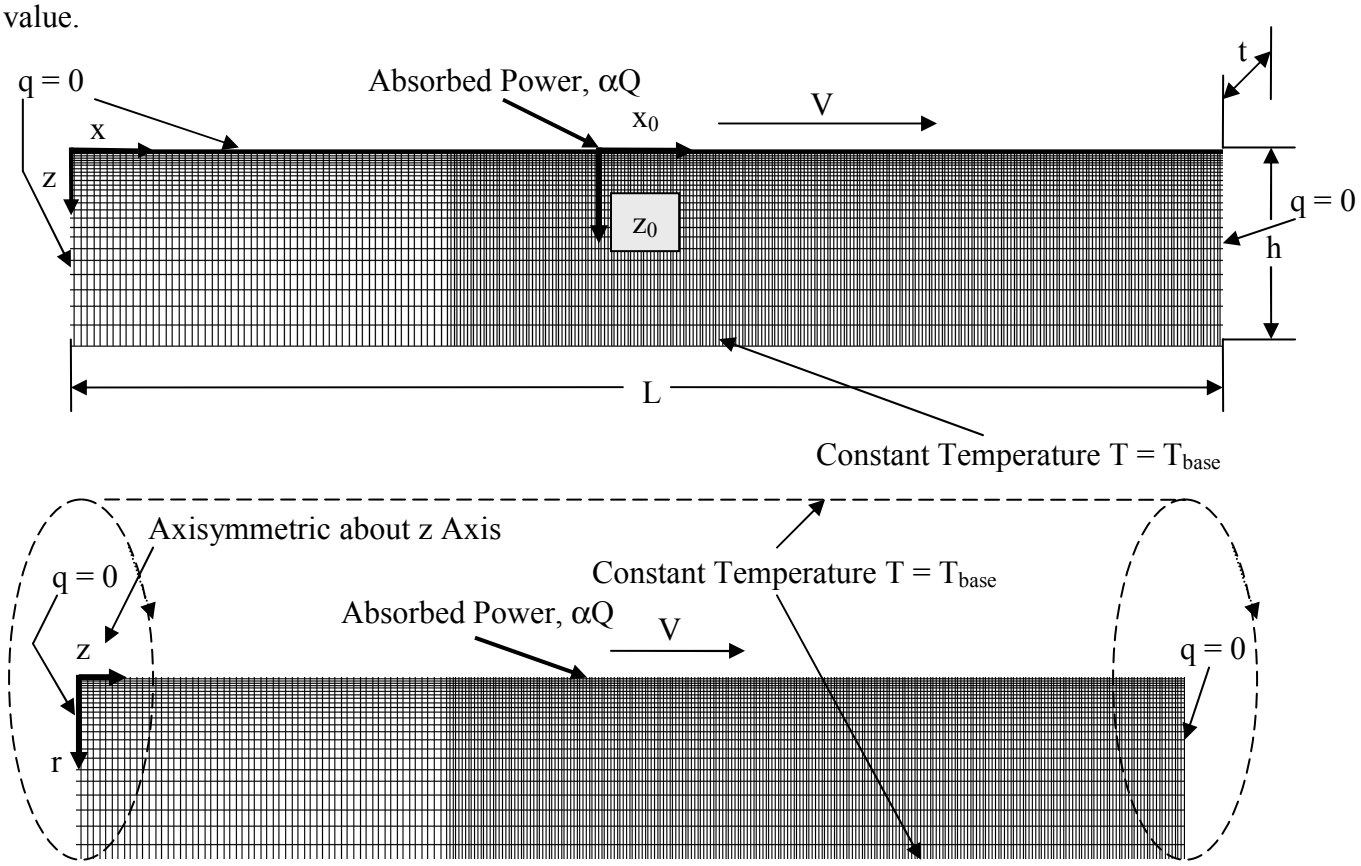

Figure 2 Finite Element Meshes with Boundary Conditions for Thin Wall and Bulky Part Simulations

Process Map Approach: The process scaling research described herein builds upon previously developed process map concepts. A process map for melt pool length for a thin-walled structure traversed by a concentrated laser heat source has been developed by Vasinonta et al. [2, 3]. As suggested by the Rosenthal [12] solution for a point heat source moving across a (2-D) half-space, a process map for melt pool length is represented through three dimensionless variables: the normalized melt pool length ($\bar{l}$), the normalized substrate height ($\bar{h}$) and the normalized melting temperature ($\bar{T}_m$) which are defined as follows:

$$\bar{l} = \frac{l}{2k/\rho cV},\ \bar{h} = \frac{h}{2k/\rho cV} \text{ and } \bar{T}_m = \frac{T_m - T_{base}}{\alpha Q/\pi kt}. \quad (2)$$

In eq. (2), ρ, c and k are the density, specific heat and thermal conductivity, respectively. If thermal properties are temperature-independent and latent heat effects are not modeled, results from the analysis of a concentrated heat source moving over a thin-walled structure of finite height, h, can be represented as a single surface plotted on three coordinate axes of $\bar{l}$, $\bar{h}$ and

$\overline{T}_m$. This forms the basis of a process map approach for analyzing the laser deposition of thin-walled structures.

A process map for deposition of thin-walled structures of 304 stainless steel via the LENS™ process can be constructed using results from temperature-dependent thermal simulations including latent heat effects if the following procedures are followed:

1. Properties at 1000 K are used in the normalizations.
2. For cases involving a change in preheat, a linear change in thermal conductivity with preheat temperature (in deg. C) is assumed, given by k = 24.3 + 0.013(T_{base}-30) W/(mK).
3. For predicting steady-state melt pool lengths resulting from a change in process variables, wall thickness is assumed to scale proportionally with melt pool length. The melt pool length/wall thickness scaling is assumed to be unaffected by velocity.

The third assumption is necessary because the wall thickness, t, is included in the normalized variable $\overline{T}_m$ used in the process map. This requires that some assumption be made regarding the relationship between melt pool length and wall thickness. It also means, however, that within the limits of assumption #3 and given a value of t from a single experiment, the process map can be used to predict not only melt pool length as a function of process variables, but also wall thickness. For process variables of laser velocity, laser power wall height and preheat temperatures of interest for the LENS™ process, thermal simulation results normalized using the rules above roughly fall on a single surface plotted on three coordinate axes of $\overline{l}$, $\overline{h}$ and $\overline{T}_m$. The variability of results due to temperature-dependent properties is +/-6.5% or less.

An analogous approach has been taken to construct process maps for the deposition of bulky parts [6]. For such structures, the dimensionless variables are:

$$\overline{d} = \frac{d}{2k/\rho cV},\ \overline{h} = \frac{h}{2k/\rho cV} \text{ and } \overline{T}_m = \frac{T_m - T_{base}}{\alpha Q/\pi k\left(\rho cV/4k\right)}, \tag{3}$$

where melt pool depths are considered instead of melt pool lengths and the nondimensionalization for $\overline{T}_m$ no longer includes a thickness, t. It should be noted that the $\overline{T}_m$ definition cited above differs by a factor of two from the bulky part $\overline{T}_m$ definition used in the study of microstructure in reference [7]. Normalization procedures needed to collapse thermal simulation results for the LENS™ process onto a single surface in 3-D nondimensional variable space are:

1. Properties of SS304 at 1100 K are used in the normalizations.
2. For cases involving a change in preheat, a linear change in thermal conductivity with preheat temperature (in deg. C) is assumed, given by k = 25.9 + 0.013(T_{base}-30) W/(mK).

If these rules are followed, the variability in melt pool depth results is also within +/-6.5%.

Targeted Manufacturing Process:

A laser processing facility is currently under development within the Advanced Materials Processing Center at the South Dakota School of Mines and Technology for use in not only net shape manufacturing but also welding, micro-machining, surface treatment and other

applications. The system consists of a 3 kW Nd:YAG laser with a robotic positioning system, dual powder feeders and geometric, temperature and position sensing capabilities. It has been tested for net shape manufacturing applications through the building of a series of thin-walled structures deposited using laser powers from 450 W to 900 W. Laser velocities of interest range from 10 to 20 mm/s. Because the power range of the laser at the AMP Center is significantly larger than that for the 500 W LENS^{TM} system, the development of this new facility offers a unique opportunity for testing the applicability of a process map approach on multiple process size scales.

Process Scaling for Thin-Walled Structures

Process Maps for Multiple Process Scales: In order to analyze the effects of process scaling, laser powers of 123 W to 2700 W (αQ from 43 W to 945 W assuming a value of $\alpha = 0.35$) were divided into two power ranges. The high power range is from 430 W to 2700 W (αQ from 150 W to 945 W). The low power range is based on the LENS™ process and has powers ranging from 123 W to 471 W (αQ from 43 W to 165 W).

As in earlier process map work, a single experimental value of the wall thickness, t, is needed to predict values of *l* and t as a function of process variables. A prediction of melt pool length, *l*, for the experiment having a known value of t yields a value of *l*/t that is used in all subsequent predictions. Also, as in earlier work, prediction of melt pool length and wall thickness using the process map must be done iteratively. For example, a larger value of αQ results in a new (smaller) value of $\overline{T}_m$. That smaller value of $\overline{T}_m$ results in a new (larger) value of *l*, and, given a value of *l*/t, a larger value of t. The larger value of t yields a slightly larger value of $\overline{T}_m$. This again leads to new values of *l* and t. These calculation steps are repeated until *l* and t stop changing significantly. Results have been extracted from thin wall numerical models for a $\overline{T}_m$ range of 0.36 to 2.7. Iterative calculation of melt pool lengths and thicknesses using V = 5.93 to 9.31 mm/s for LENS^{TM} and V = 10 to 20 mm/s for the AMP process yields ranges of $\overline{T}_m$ for the two power ranges that are within this range.

Figures 3 and 4 provide plots of $\bar{l}$ vs. $\overline{T}_m$ over the full range of $0.36 \leq \overline{T}_m \leq 2.7$ applicable to the LENS^{TM} and AMP Center processes. Results are for tall walls ($\bar{h}$ large). Data plotted in the low range of powers (large values of $\overline{T}_m$) reproduces existing process map data for LENS^{TM} for V = 7.62 mm/s. Data for smaller values of $\overline{T}_m$ is new and relates to power ranges and velocities appropriate for the AMP Center process. Figure 3 gives results for a value of T_{base} = 303 K and Figure 4 gives results for an upper bound value of T_{base} = 673 K. In both cases, results are given for the upper and lower bounds of V = 10 mm/s and V = 20 mm/s for the high power ranges (applicable to the AMP Center process). Results for V = 15 mm/s (not shown) fall between the results for the upper and lower values of velocity.

The variability in results plotted in Figs. 3 and 4 is confined to +/-3.5% in the AMP power range if the following procedures for applying the process map are followed:

1. Properties at a normalization temperature T_{norm} = 889 K are used in the normalizations.
2. For cases involving preheating, a linear change in thermal conductivity with a preheat temperature (in deg. C) is assumed, given by $k = 22.5 + 0.0058(T_{base}-30)$ W/(mK).

3. For predicting steady-state melt pool lengths resulting from a change in process variables, wall thickness is assumed to scale proportionally with melt pool length.

In other words, the process map approach can be applied over multiple process size scales by simply changing the normalization temperature in step 1 and the terms in the equation in step 2 with changes in power range.

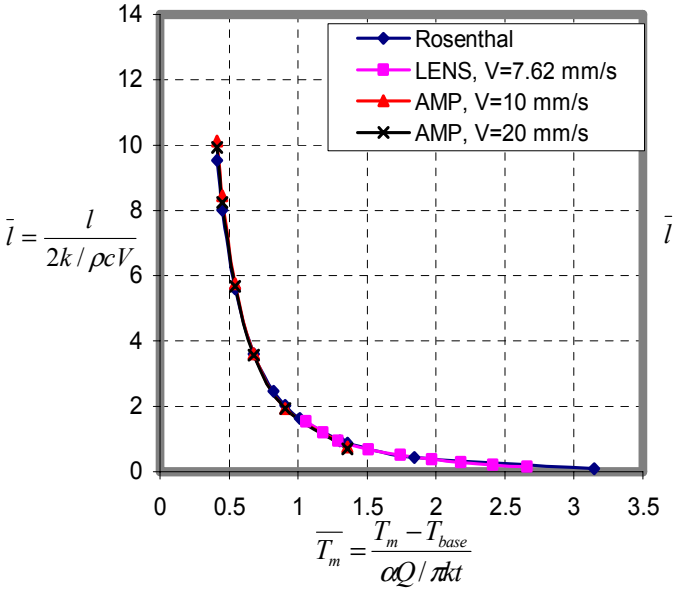

Figure 3 Comparison of Normalized Thin Wall Numerical Predictions with the Rosenthal Solution over the Full Range of $\overline{T_m}$ (T_{base} = 303 K).

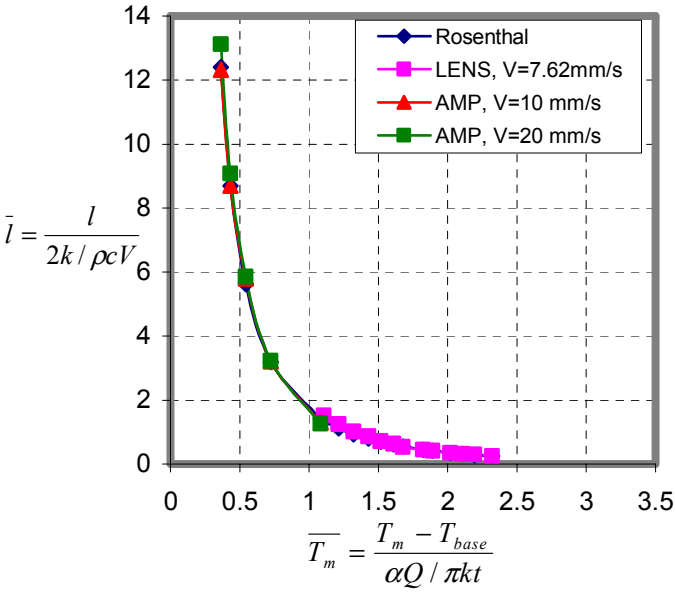

Figure 4 Comparison of Normalized Thin Wall Numerical Predictions with the Rosenthal Solution over the Full Range of $\overline{T_m}$ (T_{base} = 673 K).

Application of the Results: Figure 5 shows a plot of predicted and measured wall thicknesses vs. αQ. Measured values are from the AMP Center process for V = 20 mm/s and are shown as large data points. Predictions as a function of αQ and for V = 20 mm/s are shown as plotted lines with small data points. Two sets of predictions are presented. The top line represents process map predictions using an experimental value of t from the LENS™ process for αQ = 105 W and V = 7.62 mm/s to obtain a value of *l*/t = 1.05. Although the trends in the experiments are captured by these predictions, the predicted values are larger than the experimental values. This difference can be explained by the use of a value of *l*/t determined from experiments at a significantly lower velocity than was used in the AMP experiments. This ratio will, in fact, increase with an increase in velocity. The second set of predictions (the lower line) was generated from the same process map results (Figure 3), but with a value of t from the AMP process for αQ = 210 W and V = 14 mm/s used to obtain a value of *l*/t = 1.67. These predictions agree quite well with the available experimental data. Furthermore, the predictions for larger powers could be a useful tool in reducing the number of experiments needed to characterize the AMP process.

Process Robustness: Process robustness has been assessed by determining the sensitivity of melt pool size to changes in power and velocity for the two power ranges considered in this research. Figure 6 summarizes the thin wall process robustness results. The Rosenthal solution and appropriate normalization rules for each power range and a base temperature of T_{base} = 303 K were used to generate the plotted data.

To quantify the sensitivity of melt pool size to changes in power, low, middle and high power values within the LENS™ and AMP process power ranges were used as initial power levels. The initial LENS™ and AMP powers were αQ = 43, 104 and 165 W and αQ = 150, 548 and 945 W, respectively. The percent change in melt pool length due to power increases of up to 20% were then determined. To measure the effect of laser velocity, power change calculations were performed at three different speeds for each power range: 5.93, 7.62 and 9.31 mm/s for LENS™, and 10 15 and 20 mm/s for the AMP process.

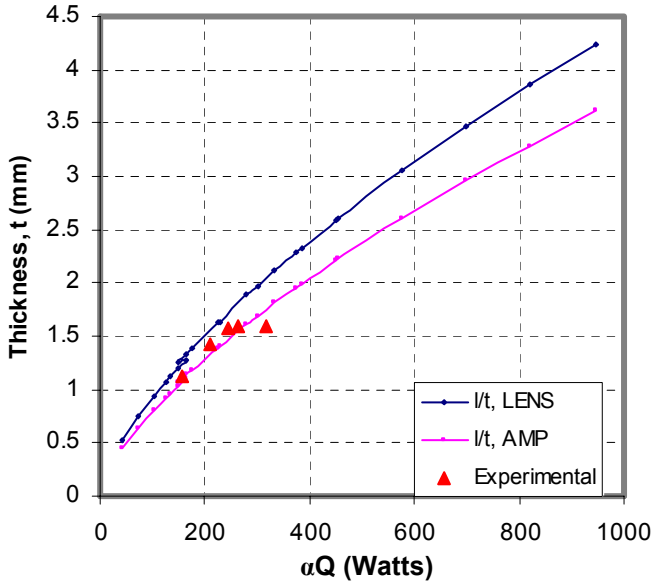

Figure 5 Comparison of Experimental and Predicted Thicknesses as a Function of αQ (α = 0.35)

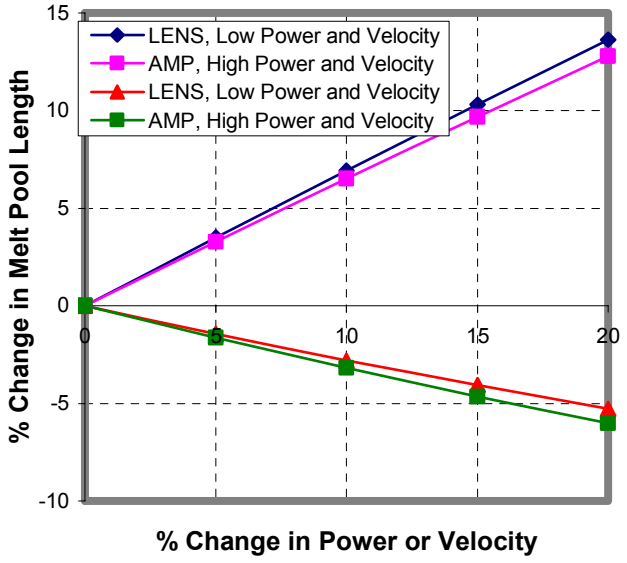

Figure 6 Process Robustness for Thin Walls for Changes in Power or Velocity

The plot in Figure 6 presents this information as two curves defining the upper and lower bounds of results due to power changes for both processes over all operating velocities. The LENS™ process operating at αQ = 43 W (minimum power, maximum $\overline{T}_m$) and the lowest velocity (V = 5.93 mm/s) yields the upper bound curve, while the AMP process operating at αQ = 945 W (maximum power, minimum $\overline{T}_m$) and the highest velocity (V = 20 mm/s) yields the lower bound curve. There is a maximum 6.6% difference between the AMP and LENS™ results indicating that process robustness with respect to power changes is nearly independent of process size scale. Interestingly, this convergence of results for all power ranges does not occur unless increases in wall thickness due to increases in melt pool size are accounted for. Another interesting feature of the results plotted in Fig. 6 is the nearly linear relationship between melt pool length and percent change in power. This is despite $\bar{l}$ vs. $\overline{T}_m$ plots that are highly nonlinear (see Figs. 3 and 4). This is due to the relatively small changes in $\overline{T}_m$ that are involved in generating the power change data in Fig. 6, which render $\bar{l}$ vs. $\overline{T}_m$ behavior approximately linear.

Sensitivities to velocity changes were obtained in a manner analogous to the determination of power sensitivity. Melt pool lengths as a function of changes in velocity were calculated for three initial velocities and at three operating powers within each power range. The velocity change results shown in Figure 6 are the upper and lower bounds of the curves for both

the LENS™ and AMP ranges. The LENS™ results operating at low power and low velocity yield the lower bound in sensitivity, while the AMP process operating at the highest power and high velocity yields the upper bound. There is a maximum 14% difference between AMP and LENS™ results, indicating that process robustness with respect to changes in velocity is somewhat dependent on process size.

The data plotted in Fig. 6 also indicates that the magnitudes of the slopes of the power change curves are approximately three times those of the velocity change curves. Thus, for the consistent construction of thin-walled structures, it is more important to minimize fluctuations in power than fluctuations in velocity to maintain a desired melt pool geometry. Conversely, if a change in melt pool size is needed, changing laser power is more effective than changing laser velocity.

Process Scaling for Bulky Structures

Process Maps for Multiple Process Scales: Steps analogous to those taken to analyze thin-walled structures are followed here, except that for bulky structures, a value of $\alpha = 0.70$ is used to determine $\overline{T}_m$ ranges. The use of a value of $\alpha = 0.70$ is based on agreement between numerical model predictions and measurements of melt pool width for the LENS™ process. It is believed that in the building of bulky parts, power absorption by the powder streams acts to increase the ability of the substrate to absorb laser power by roughly a factor of 2. Experiments involving laser glazing of bulky structures (passing of a laser over the surface without powder deposition) have not shown this effect. This assumed value of α only affects the ranges of absorbed laser powers analyzed. Results are presented in terms of αQ, and any other value of α can be used when applying results to predict melt pool sizes. In order to analyze the effects of process scaling, laser powers of 123 W to 2700 W (αQ from 86 W to 1890 W assuming a value of α = 0.70) were divided into two power ranges. The upper range, based on the AMP process, is from 430 W to 2700 W (αQ from 300 W to 1890 W). The lower range is based on the LENS™ process and has powers ranging from 123 W to 471 W (αQ from 86 W to 330 W).

Figures 7 and 8 provide plots of $\overline{d}$ vs. $\overline{T}_m$ ($\overline{h}$ large) over the full range of $0.059 \leq \overline{T}_m \leq 5.82$ applicable to the LENS™ and AMP Center processes. Figure 7 gives results for a value of T_{base} = 303 K and Figure 8 gives results for T_{base} = 673 K. In both cases, results for the AMP process (which is new data) are given for the upper and lower bounds of V = 10 mm/s and V = 20 mm/s. Properties at 1000 K are used in the normalizations. For the cases of T_{base} > 30 C, the dependence of conductivity on preheat temperature T_{base} is taken as:

$$k = 24.3 + .0013(T_{base}-30) \quad (W/(mK)) . \qquad (4)$$

As with the thin-walled geometry, normalization by properties at a lower temperature has allowed results from larger-scale processes to be collapsed onto a single curve. Combining the data of Figs. 7 and 8 reveals that variability of results in the AMP power range due to latent heat and thermal property temperature dependence can be confined to +/-3%.

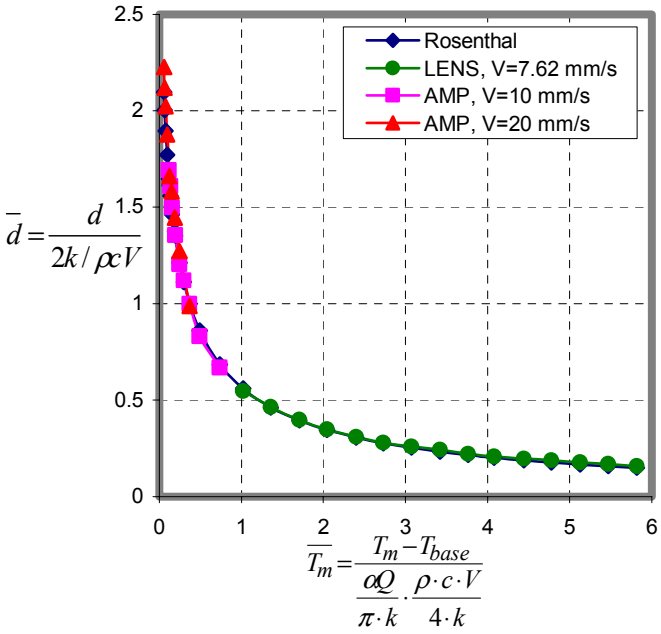

Figure 7 Comparison of Normalized Bulky Part Numerical Predictions to the Rosenthal Solution over the Full Range of $\bar{T}_m$, using a Pre-Heat Temperature T_{base} = 303K.

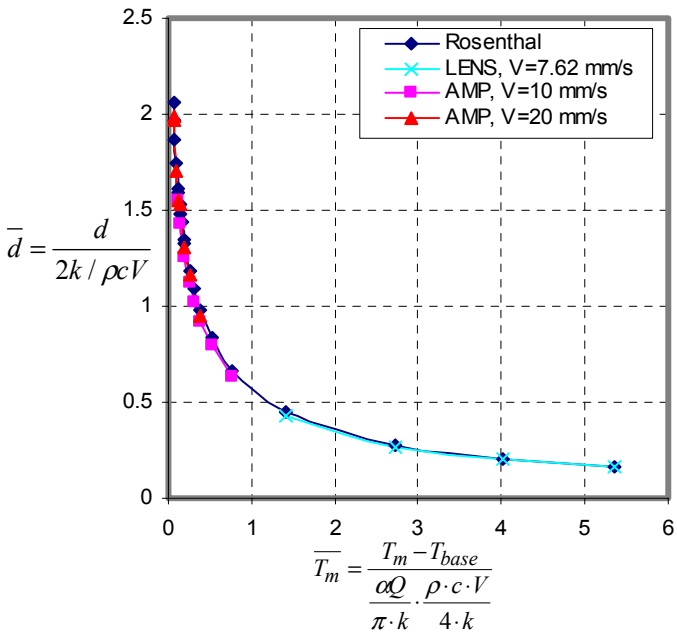

Figure 8 Comparison of Normalized Bulky Part Numerical Predictions to the Rosenthal Solution over the Full Range of $\bar{T}_m$ using a Pre-Heat Temperature T_{base} = 673 K.

Process Robustness: Figures 9 and 10 present plots of melt pool depth changes due to power changes (Fig. 9) and velocity changes (Fig. 10) analogous to the single plot for thin walled structures provided in Fig. 6. Analogous to the thin-wall case, the 3-D Rosenthal solution with a base temperature of T_{base} = 303 K has been used as a basis for all calculations. Low, mid-level and high power values are all twice those used to generate Fig. 6, consistent with a value of α = 0.70. Low, mid-level and high velocities for each process are unchanged.

The plot in Figure 9 shows sensitivity to changes in power as a set of six curves, each corresponding to one value of initial power. The curve is drawn through the data for the mid-level velocity for each case (V = 7.62 mm/s for the LENS™ power range and V = 15 mm/s for the AMP power range). Values for the other two velocities are plotted as data points only. Unlike the results for thin walls, there is a substantial dependence of results on initial power level and velocity. However, the plot in Figure 9 indicates that the smaller-scale LENS™ process is generally more sensitive to power fluctuations. Overall, sensitivity decreases with an increase in initial power (decreasing initial $\bar{T}_m$). Increases in operating velocity for a specific initial power value result in decreased sensitivity to changes in power. As in the results for thin walls, curves are nearly linear, due to the relatively small changes in $\bar{T}_m$ involved.

Sensitivities to velocities are characterized in Fig. 10. Melt pool depths as a function of changes in velocity were recorded at the three different velocities and at three operating powers within each range. The display of data is analogous to that for Fig. 9. The plot of Fig. 10 shows that although there is significant variability of results with power and velocity, the AMP process is more sensitive to fluctuations in velocity than the LENS™ process. Overall, increases in operating power for a specific velocity level result in increased sensitivity to changes in velocity.

In contrast to the thin wall case, the results in Figures 9 and 10 suggest that, for the manufacture of bulky components, the sensitivity of laser-based additive manufacturing processes to changes in either laser power or laser velocity are significantly dependent on process size scale. The larger-scale AMP process is less sensitive to (more robust with respect to) fluctuations in power. The smaller-scale LENS™ process is more robust with respect to fluctuations in velocity. Results also suggest that when working exclusively in the smaller-scale LENS™ range, it is more important to control fluctuations in power rather than velocity. When operating in the larger AMP range, control of fluctuations in velocity and power are roughly equally important.

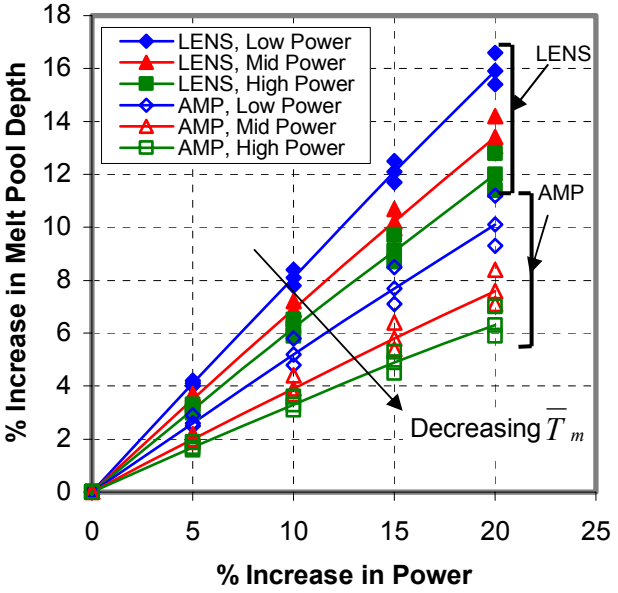

Figure 9 Process Robustness for Bulky Parts for Changes in Laser Power

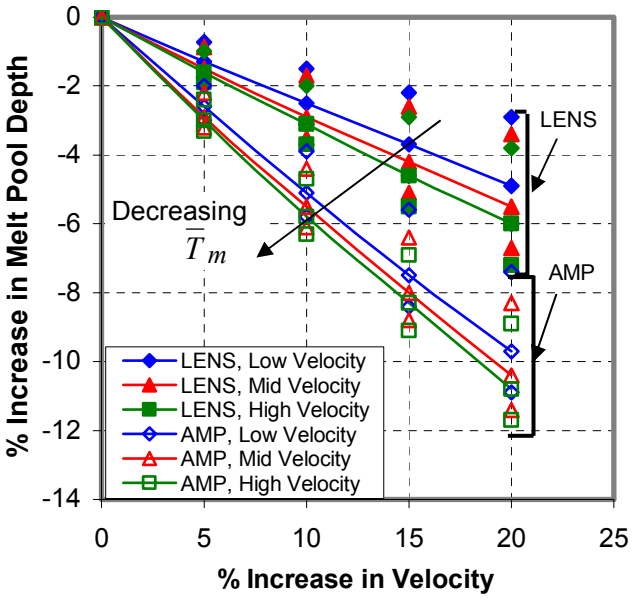

Figure 10 Process Robustness for Bulky Parts for Changes in Laser Velocity

Summary and Conclusions

In this study, process map approaches previously developed for application to the LENS™ process have been extended to predict steady-state melt pool sizes for larger-scale processes. This allows the easy prediction of melt pool size for any combination of laser powers, laser velocities and part preheat temperatures. Process scaling predictions of wall thicknesses have been made for the full power range of a large-scale process currently under development and predictions have compared well to thicknesses measured to date. A study of the sensitivity of melt pool size to changes in process variables suggests that, due to changes in wall thickness, process robustness is not a strong function of process size for the deposition of thin walls. In contrast there is a large variation in process robustness with process size for the deposition of bulky features.

Acknowledgements

Modeling research at Carnegie Mellon is supported by the National Science Foundation Division of Design, Manufacture and Industrial Innovation, through the Materials Processing and Manufacturing Program, award number DMI-0200270. Manufacturing research at the AMP

Center is supported by the U.S. Army Research Laboratory and the U.S. Army Office under grant number DAAD 19-02-2-001. The authors would like to thank Dave Alexander and Ralph Anderson of Pratt & Whitney for their insights and effort in guiding the industrial applications of this research.

References

1. Griffith, M.L., Keicher, D.M., Atwood, C.L., Romero, J.A., Smugeresky, J.E., Harwell, L.D. and Greene, D.L., 1996, "Freeform Fabrication of Metallic Components Using Laser Engineered Net Shaping (LENS^{TM})" *Solid Freeform Fabrication Proceedings*, Austin, August 1996, pp. 125-132.
2. Vasinonta, A., Beuth, J. L. and Griffith, M. L., 1999, "Process Maps for Laser Deposition of Thin-Walled Structures," *Solid Freeform Fabrication Proceedings*, Austin, August 1999, pp. 383-391.
3. Vasinonta, A., Beuth, J. L. and Griffith, M. L., 2001, "A Process Map for Consistent Build Conditions in the Solid Freeform Fabrication of Thin-Walled Structures," *Journal of Manufacturing Science and Engineering.* Vol. 123, pp. 615-622.
4. Vasinonta, A., Beuth, J.L., and Ong, R., 2001, "Melt Pool Size Control in Thin-Walled and Bulky Parts via Process Maps," *Solid Freeform Fabrication Proceedings*, Austin, August 2001, pp. 432-440.
5. Beuth, J.L. and Klingbeil, N.W., 2001, "The Role of Process Variables in Laser-Based Direct Metal Solid Freeform Fabrication," *JOM,* September 2001, pp. 36-39.
6. Vasinonta, A., 2002, "Process Maps for Melt Pool Size and Residual Stress in Laser-based Solid Freeform Fabrication," Ph.D. Thesis, Carnegie Mellon University, May 2002.
7. Bontha, S. and Klingbeil, N.W., 2003, "Thermal Process Maps for Controlling Microstructure in Laser-Based Solid Freeform Fabrication," *Solid Freeform Fabrication Proceedings*, Austin, August 2003, pp. 219-226.
8. Birnbaum, Aggarangsi and Beuth, 2003, "Process Scaling and Transient Melt Pool Size Control in Laser-Based Additive Manufacturing Processes", *Solid Freeform Fabrication Proceedings*, Austin, August 2003, pp. 328-339.
9. Aggarangsi, P., Beuth, J.L., and Gill, D.D., 2004, "Transient Changes in Melt Pool Size in Laser Additive Manufacturing Processes," *Solid Freeform Fabrication Proceedings*, Austin, August 2004 (in the current proceedings).
10. Aggarangsi, P., Beuth, J.L., and Griffith, M.L., 2003, "Melt Pool Size and Stress Control for Laser-Based Deposition Near a Free Edge," *Solid Freeform Fabrication Proceedings*, Austin, August 2003, pp. 196-207.
11. Dobranich, D. and Dykhuizen, R.C., 1998, "Scoping Thermal Calculation of the LENS^{TM} Process," Sandia National Laboratories Internal Report.
12. Rosenthal, D., 1946, "The Theory of Moving Sources of Heat and Its Application to Metal Treatments," *Transactions of ASME,* Vol. 68, 1946, pp. 849-866.